Bull. Mater. Sci., Vol. 37, No. 6, October 2014, pp. 1275–1282. © Indian Academy of Sciences.

Optimization of AZO films prepared on flexible substrates

C C HU[1,2], T W LU[1,3], C Y CHOU[4], J T WANG[4], H H HUANG[4] and C Y HSU[4,*]
[1]Institute of Biomedical Engineering, National Taiwan University, Taipei, Taiwan
[2]Department of Mechanical Engineering, Ming Chi University of Technology, Taipei, Taiwan
[3]Department of Orthopaedic Surgery, School of Medicine, National Taiwan University, Taipei, Taiwan
[4]Department of Mechanical Engineering, Lunghwa University of Science and Technology, Taoyuan, Taiwan

MS received 10 April 2013; revised 26 July 2013

Abstract. **Transparent conductive Al_2O_3-doped zinc oxide (in AZO, Al_2O_3 content is ~ 2 wt%) thin films are deposited on flexible polyethylene terephthalate (PET) substrates, using radio frequency (rf) magnetron sputtering. The Taguchi method with an L_9 (3^4) orthogonal array, a signal-to-noise ratio and analysis of variance (ANOVA) was used to determine the performance characteristics of the coating operations. Using grey relational analysis, the optimization of these deposition process parameters for AZO thin films with multiple characteristics was performed. The electrical resistivity of AZO/PET films is reduced from $2·6 \times 10^{-2}$ to $5·5 \times 10^{-3}$ Ω-cm and the visible range transmittance is > 83%, using the grey relational analysis. ANOVA results for the grey relational grade indicate that rf power and working pressure are the two most influential factors. The effect of the rf power (in the range from 30 to 70 W) and the argon working pressure (in the range from 0·90 to 1·1 Pa) on the morphology and optoelectronic performance of AZO films are also investigated. An analysis of the influence of the dominant parameters in the optimal design region is helpful for adjustment of the coating parameters.**

Keywords. **Flexible substrates; Al_2O_3-doped zinc oxide; magnetron sputtering; grey relational analysis.**

1. Introduction

Transparent conductive oxide films have attractive optical–electrical characteristics, such as visible transmittance > 80% and a resistivity < 10^{-3} Ω-cm. They are extensively used in various transparent optoelectronic devices (LED, OLED, PLED, LCD, PDP or solar cells) (Jin *et al* 2000), piezoelectric devices and surface acoustic wave devices (Kassis and Saad 2003). Indium tin oxide (In_2O_3: Sn, ITO), tin oxide (SnO_2) and zinc oxide (ZnO) are the best-known materials for typical transparent conductive films. The optical transmittance of ITO films of thickness between 1000 and 1500 Å can be > 90%, but their targets are expensive and toxic. ZnO and SnO_2 films are of interest because of their low cost and high crystallinity (Miyazaki *et al* 1997). Compared with SnO_2 films, ZnO films are more easily etched to form fine electrodes. With the properties of low carrier concentration and high resistivity, non-doped ZnO films are usually used in piezoelectric applications. In order to improve the conductivity of ZnO films, Al, Ga and In have been found to be effective dopants for carrier generation (Agashe *et al* 2004; Kao *et al* 2010). Of these, impurity-doped zinc oxide films, Al-doped zinc oxide (AZO) thin film has excellent characteristics (Lin *et al* 2009). Several deposition techniques have been used to fabricate AZO films, such as sol–gel techniques, spray pyrolysis (Paraguay *et al* 2000), chemical vapour deposition, pulsed laser deposition and magnetron sputtering (Szyszka 1999; Yu *et al* 2005a, b; Chen and Hsu 2008). The sputtering processes are the most common techniques for preparation of AZO films, because of good surface roughness, low cost and low working temperatures.

Transparent conductive oxide thin films are deposited on glass substrates for high transparency and conductivity (Moon *et al* 2007; Rim *et al* 2008). However, glass is too heavy, fragile and brittle for manufacturing. Flexible polymer substrates are remarkably flexible, lightweight and easy to handle. Recently, they are used in electronic devices, such as flat panel display devices. AZO (Al_2O_3 content is about 2 wt% (Chung *et al* 2005) films prepared on flexible polyethylene terephthalate (PET) substrates using radio frequency (rf 13·56 MHz) magnetron sputtering are reported in this study. The transparent conductive AZO thin films are deposited on PET, which gives high visible transparency and high conductivity. A lower working temperature is necessary because the organic material, PET, has poor thermal stability (Fortunato *et al* 2003).

In the literature, many deposition factors such as power mode, rf power, total gas working pressure, oxygen ratio,

*Author for correspondence (cyhsu@mail.lhu.edu.tw)

Table 1. Deposition conditions and settings for control factors.

Substrate	PET (T60, area 25 × 25 mm, thickness 1 mm)
Target	AZO ($ZnO : Al_2O_3$, 98 : 2 wt%, 99·995% pure)
Gas	Argon (99·995% purity)
Base pressure	$5·3 \times 10^{-4}$ Pa
Substrate-to-target distance	90 mm
Substrate rotate speed	20 rpm

Symbol	Control factor	Level 1	Level 2	Level 3
A	rf power (W)	50	85	120
B	Working pressure (Pa)	0·8	1	1·2
C	Substrate temperature (°C)	room	90	150
D	Deposition time (min)	20	35	50

bias voltage, annealing temperature and plasma treatment deposition time (Pei *et al* 2006; Fernández *et al* 2009; Tseng *et al* 2011) influence the properties using rf magnetron sputtering to prepare transparent conductive AZO thin films on flexible PET substrates. Among these factors, the rf power, working pressure, substrate temperature and deposition time have most significant effects on the performance of deposition rate, resistivity and transmittance (Lin *et al* 2009; Tseng *et al* 2011).

A grey-Taguchi analysis has been successfully used to optimize the coating parameters for multiple characteristics using a Taguchi experimental design, signal-to-noise (S/N) ratio, analysis of variance (ANOVA) and grey relational analysis (Chen and Hsu 2008; Hsu and Tsang 2008). However, effect of the dominant parameters in the optimal design region is seldom discussed. In this paper, an L_9 (3^4) orthogonal array with four columns (including rf power, working pressure, substrate temperature and deposition time) and nine rows are used. The influence of the dominant parameters on the performance of the optimal design using grey-Taguchi analysis are studied. The effects of AZO films on structural, electrical and optical properties are also investigated.

2. Experimental

AZO transparent conducting films were deposited on PET (T60 with an area of 25 × 25 mm and a thickness of 1 mm) substrates, using rf magnetron sputtering with a base pressure of $5·3 \times 10^{-4}$ Pa. AZO ($ZnO : Al_2O_3$, 98 : 2 wt%, 99·995% pure) was a commercially available hot-pressed and sintered target, with a diameter of 2 in and a thickness of 0·25 in. All of PET substrates were ultrasonically cleaned in acetone, rinsed with deionized water and dried in nitrogen. The substrate-to-target distance was 90 mm and the rotational speed of the substrate was maintained at 20 rpm, in order to ensure good surface morphology. The deposition conditions and the settings for the control factors are shown in table 1. Before deposition, the target was pre-sputtered at a constant rf power of 20 W for 10 min to remove any contamination.

After deposition, the electrical resistivity was measured by the four-point probe method (Mitsubishi chemical MCP-T600). The optical transmittance measurement was performed using a UV–Vis spectrophotometer in the wavelength range of 300–800 nm. The film thickness was measured using a surface profilometer (α-step, AMBIOS XP-1). A field emission scanning electron microscope (SEM, JEOL, JSM-6500F) was used to analyse the surface morphologies and an atomic force microscope (AFM, PSIA-XE-100) provided topographic images. The structural properties were determined using X-ray diffraction (XRD, Rigaku-2000 X-ray generator), using CuKα radiation (λ = 1·54056 Å) with an angle incidence of 1°. The grain sizes of the films were calculated from XRD data, using the Debye–Scherrer formula.

3. Grey relational analysis and optimization

Grey relational analysis is a method for analysing the relationship between sequences using less data with multiple factors and is considered helpful to statistical regression analysis. Based on the grey system theory, the grey relational analysis can be used to solve complicated interdependence of parameters among multiple performance characteristics effectively (Deng 1989; Kuo *et al* 1998; Tarng *et al* 2002; Chen and Hsu 2008; Hsu and Tsang 2008). In this paper, a Taguchi experimental design and grey relational analysis were used to clarify the effect of various sputtering factors, in order to obtain low resistivity, good visible transparency and a high deposition rate, i.e. to optimize the design of the process for the deposition of the transparent conductive AZO thin film.

Taguchi approach is a powerful design tool for high-quality systems (Phillip 1989). To conduct the Taguchi method efficiently, an orthogonal array is employed for the design of experiments. The number of experiments, N_{Taguchi}, is calculated as follows

$$N_{\text{Taguchi}} = 1 + \sum_{i=1}^{N_p} (L_i - 1), \qquad (1)$$

where N_p is the number of parameters and L_i is the number of levels. In this study, there are 4 parameters and

3 levels; therefore, the number of experiments are 1 + 4*(3 – 1), i.e. nine experiments.

3.1 *Analysis of S/N ratio*

In order to quantify the variation in the experiments, generically different signal-to-noise (*S*/*N*) ratios were employed, depending on the particular type of characteristics involved. These included 'lower is better' (LB), 'nominal is best' (NB) and 'higher is better' (HB). *S*/*N* ratios were calculated using the following equations

$$\eta = 10\log(S/N \text{ ratio}) = 10\log\frac{1}{\sigma^2} = -10\log\sigma^2, \quad (2)$$

$$\text{HB}: \sigma^2 = \frac{1}{n}\left(\frac{1}{y_1^2} + \frac{1}{y_2^2} + \cdots + \frac{1}{y_n^2}\right), \quad (3)$$

$$\text{LB: LB}: \sigma^2 = \frac{1}{n}(y_1^2 + y_2^2 + \cdots\cdots + y_n^2), \quad (4)$$

where η denotes the calculated value of *S*/*N* ratio (unit: d*B*). y_n represents the measured experimental value and n is a repeated number. A larger set of y_n squares in the HB (3) induces a small value for σ^2 and a large *S*/*N* ratio value η, in (2). Good visible transmittance and deposition rate are in the category of higher-the-better performance characteristics and electrical resistivity is lower the better. The mean *S*/*N* ratio for each level of the process parameters is summarized in the *S*/*N* response table.

3.2 *Analysis of variance*

An ANOVA and the *F*-test are used to analyse the experimental data as follows

$$S_{\text{m}} = \frac{\left(\sum \eta_i\right)^2}{9}, \; S_{\text{m}} = \sum \eta_i^2 - S_{\text{m}}, \quad (5)$$

$$S_A = \frac{\left(\sum \eta_{Ai}^2\right)^2}{N} - S_{\text{m}}, \; S_{\text{E}} = S_{\text{T}} - \sum S_A, \quad (6)$$

$$V_A = \frac{S_A}{f_A}, \quad F_{A0} = \frac{V_A}{V_{\text{E}}}, \quad (7)$$

where η_i is the η value for each experiment (i = 1–9), S_{m} is the square of the sum due to the means and S_{T} is the sum of the squares due to the total variation. S_A is the sum of the squares due to parameter A, η_{Ai} is the sum of the ith level of parameter A (i = 1, 2, 3), N is the repeating number of each level of parameter, A and S_{E} is the sum of the squares due to error. The values, f_A, V_A, V_{E} and F_{A0}, are the degree of freedom, the variance and the *F*-test value for parameter, A, respectively.

3.3 *Grey relational analysis*

Grey relational analysis was used to determine the complicated relationships between the multiple performance characteristics for AZO/PET deposition. The grey relational coefficient is

$$r(x_0(k), x_i(k)) = \frac{\min\limits_i \min\limits_k |x_0(k) - x_i(k)| + \xi \max\limits_i \max\limits_k |x_0(k) - x_i(k)|}{|x_0(k) - x_i(k)| + \xi \max\limits_i \max\limits_k |x_0(k) - x_i(k)|}, \quad (8)$$

where $x_i(k)$ is the normalized value of the kth performance characteristic in the ith experiment and ξ is the coefficient adjusted between 0 and 1, according to the actual system requirements. In this paper, $\xi = 0{\cdot}5$, because all of the parameters are equally weighted. The grey relational grade, defined as follows, is a weighing-sum of the grey relational coefficient

$$r(x_0, x_i) = \frac{1}{N}\sum_{k=1}^{N} r(x_0(k), x_i(k)), \quad (9)$$

Table 2. Experimental results and *S*/*N* ratios for deposition rate, resistivity and transmittance of the AZO/PET (the experiments were repeated twice).

	Factors				Deposition rate (nm/min)			Resistivity (10^{-3} Ω-cm)			Transmittance (%)		
Exp.	A	B	C	D	DP_1	DP_2	*S*/*N* (dB)	R_1	R_2	*S*/*N* (dB)	T_1	T_2	*S*/*N* (dB)
1	1	1	1	1	4·1	4·2	12·36	22·2	21·9	–26·87	77·3	75·6	37·67
2	1	2	2	2	4·2	4·2	12·47	26·6	25·8	–28·37	88·6	85·4	38·79
3	1	3	3	3	5·0	5·2	14·15	5·73	5·65	–15·10	79·9	80·2	38·07
4	2	1	2	3	7·5	7·5	17·50	27·3	27·8	–28·80	74·1	72·8	37·32
5	2	2	3	1	6·2	6·5	16·05	37·4	36·9	–31·40	81·9	80·6	38·20
6	2	3	1	2	7·5	7·7	17·61	34·4	33·8	–30·66	79·0	77·4	37·86
7	3	1	3	2	11·7	12·2	21·54	96·6	95·4	–39·65	78·8	77·6	37·86
8	3	2	1	3	10·3	11·3	20·64	24·7	23·5	–27·64	76·7	75·6	37·63
9	3	3	2	1	10·0	10·4	20·17	46·2	45·1	–33·19	74·5	73·8	37·40

Table 3. ANOVA results for AZO/PET deposition rate, resistivity and transmittance.

Factors	*S*/*N* ratio (dB) Level 1	Level 2	Level 3	Degree of freedom	Sum of square	Variance	Contribution (*P* %)
Deposition rate							
A	12·99	17·06	20·80	2	91·40	45·70	95·29
B	17·14	16·40	17·31	2	1·42	0·71	1·48
C	16·88	16·71	17·25	2	0·46	0·23	0·48
D	16·20	17·21	17·44	2	2·63	1·32	2·75
Total				8	95·90		100
Electrical resistivity							
A	–23·45	–30·29	–33·49	2	158·01	79·00	46·56
B	–31·77	–29·14	–26·32	2	44·68	22·34	13·17
C	–28·39	–30·12	–28·72	2	5·07	2·54	1·50
D	–30·49	–32·89	–23·85	2	131·54	65·77	38·77
Total				8	339·30		100
Visible range transmittance							
A	38·17	37·79	37·63	2	0·46	0·23	28·57
B	37·62	38·20	37·78	2	0·56	0·28	34·78
C	37·72	37·84	38·04	2	0·16	0·08	9·94
D	37·75	38·17	37·67	2	0·43	0·22	26·71
Total				8	1·61		100

where N is the number of performance characteristics. The grey relational grade shows the correlation between the reference sequence and the comparability sequence. The evaluated grey relational grade fluctuates from 0 to 1. It equals 1 if these two sequences are identically coincident. The optimal combination of AZO/PET deposition parameters is obtained from grey relational analysis and a statistical analysis of variance.

4. Results and discussion

Table 2 shows the experimental results for AZO/PET sputtering process, with regard to deposition rate, resistivity and transmittance and the corresponding *S*/*N* ratios. ANOVA results, including *S*/*N* ratio, degree of freedom (DOF), sum of square, variance and contribution are presented in table 3. DOF of a specific parameter is calculated as the number of experimental levels – 1 (Osama *et al* 2009). In this study, the levels of the 4 factors are all set as 3. Therefore, the individual DOF of any factor is 2, and the total DOF of one set of the experiment is 4*(3 – 1), i.e. 8 DOF. It is seen that that the rf power has the dominant effect on the deposition rate, with a contribution ratio of almost 95·29%. The deposition rate is increased when the rf power is increased. These higher-energy particles have high surface mobility and therefore more growth takes place at the surface (Yu *et al* 2005a, b). The contribution ratios of working pressure, substrate temperature and deposition time to deposition rate are only 1·48, 0·48 and 2·70%, respectively. These shows that the deposition rate can only fluctuate within a small range, according to these control factors.

Table 4. Grey relational grade and its order for each deposition level.

Exp.	Grey relational grade	Rank
1	0·5625	4
2	0·8438	1
3	0·7468	2
4	0·5035	7
5	0·5651	3
6	0·5244	6
7	0·3842	9
8	0·5474	5
9	0·4379	8

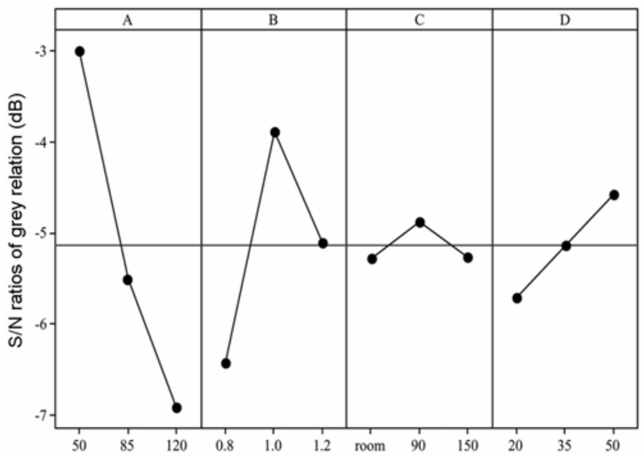

Figure 1. *S*/*N* response graph for the grey relational grade for AZO/PET deposition process. Note: A = rf power (W), B = working pressure (Pa), C = substrate temperature (°C), D = deposition time (min).

Table 5. Confirmation test for resistivity and transmittance, using the grey theory prediction design and the orthogonal array parameters.

	Orthogonal array parameter $A_1B_2C_2D_2$	Grey theory prediction design $A_1B_2C_2D_3$	Improvement rate (%)
Resistivity (10^{-3} Ω-cm)	26	5·5	78·84
Transmittance (%)	87·6	83·0	–5·25

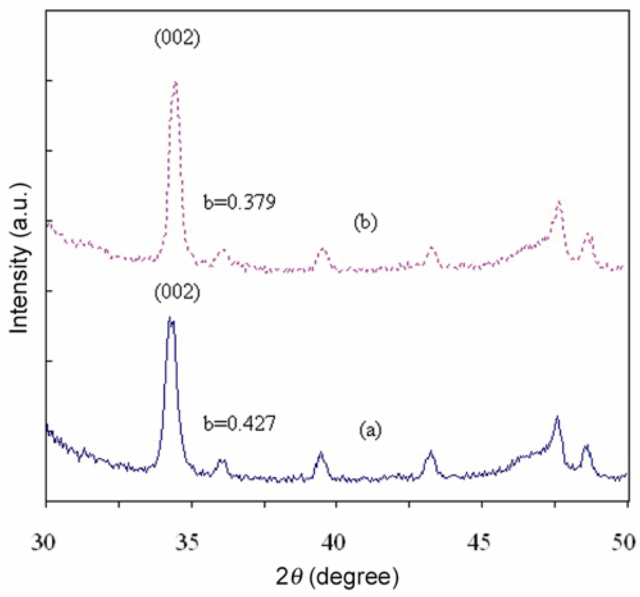

Figure 2. X-ray diffraction spectrum for AZO/PET films: (a) orthogonal array parameters and (b) grey theory prediction design (b: full-width at half-maximum FWHM).

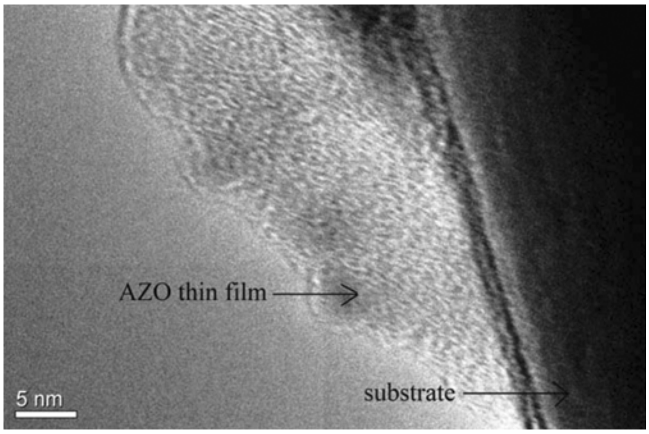

Figure 3. High-resolution TEM images of AZO thin film deposited using a grey theory prediction design.

ANOVA analysis in table 3 results show that the rf power has the dominant effect on AZO/PET electrical resistivity, with a contribution ratio of almost 46·56%, followed by deposition time with 38·77%. A lower rf power produces lower electrical resistivity. As the rf power increases, the electrical resistivity of AZO films increases. The increase in resistivity occurs because of the damage to AZO film caused by the collision of negative ions (Lee *et al* 2008). ANOVA results reveal that the working pressure dominates transmittance, with a contribution ratio of 34.78%, followed by the rf power and deposition time with 28·57 and 26·71%, respectively. Suitable values for rf power (50 W), working pressure (1 Pa) and deposition time (35 min) result in an increase in the transmittance of AZO films on PET.

4.1 *Optimal deposition parameters*

Using (7) and (8), the grey relational grade for each experiment and its order in the optimization process using L_9 orthogonal array are shown in table 4. The parameter set, $A_1B_2C_2D_2$ (50 W, 1 Pa, 90 °C, 35 min), in experiment 2 has the best multiple performance (grey relational grade 0·8438) of the nine experiments. *S*/*N* response graph for the grey relational grade shown in figure 1 shows that better multiple qualities are obtained by using the parameter set, $A_1B_2C_2D_3$ (50 W, 1 Pa, 90 °C, 50 min). The confirmed experimental results for the multiple performance characteristics of AZO/PET thin films are shown in table 5. A comparison of the grey theory prediction design ($A_1B_2C_2D_3$) with the orthogonal array process parameters ($A_1B_2C_2D_2$) shows that the electrical resistivity of AZO/PET thin films is reduced from $2{\cdot}6 \times 10^{-2}$ to $5{\cdot}5 \times 10^{-3}$ Ω-cm, which is an improvement of 78·84%. An increase in the film thickness from 170 to 258 nm leads to a slight decrease in the visible range transmittance from 87·6 to 83·0% (including PET substrate).

Figure 2 shows XRD diffraction patterns for AZO films. Using grey theory prediction design, it can be seen that the intensity of the (0 0 2) diffraction peak becomes stronger and there is a decrease in the full width at half maximum (FWHM, reduced from 0·427 to 0·379), which leads to an improvement in the crystallinity and a larger crystallite size for the films (figure 2b). Figure 3 shows high-resolution TEM images of AZO thin film deposited using grey theory prediction design. Figure 4 shows the SEM and AFM images of the films deposited with (a) orthogonal array parameters and (b) grey theory prediction design. A larger grain size (figure 4b) reduces the grain boundary scattering and increases carrier lifetime, which leads to increased conductivity, because of the increase in carrier concentration and Hall mobility (Lv *et al*

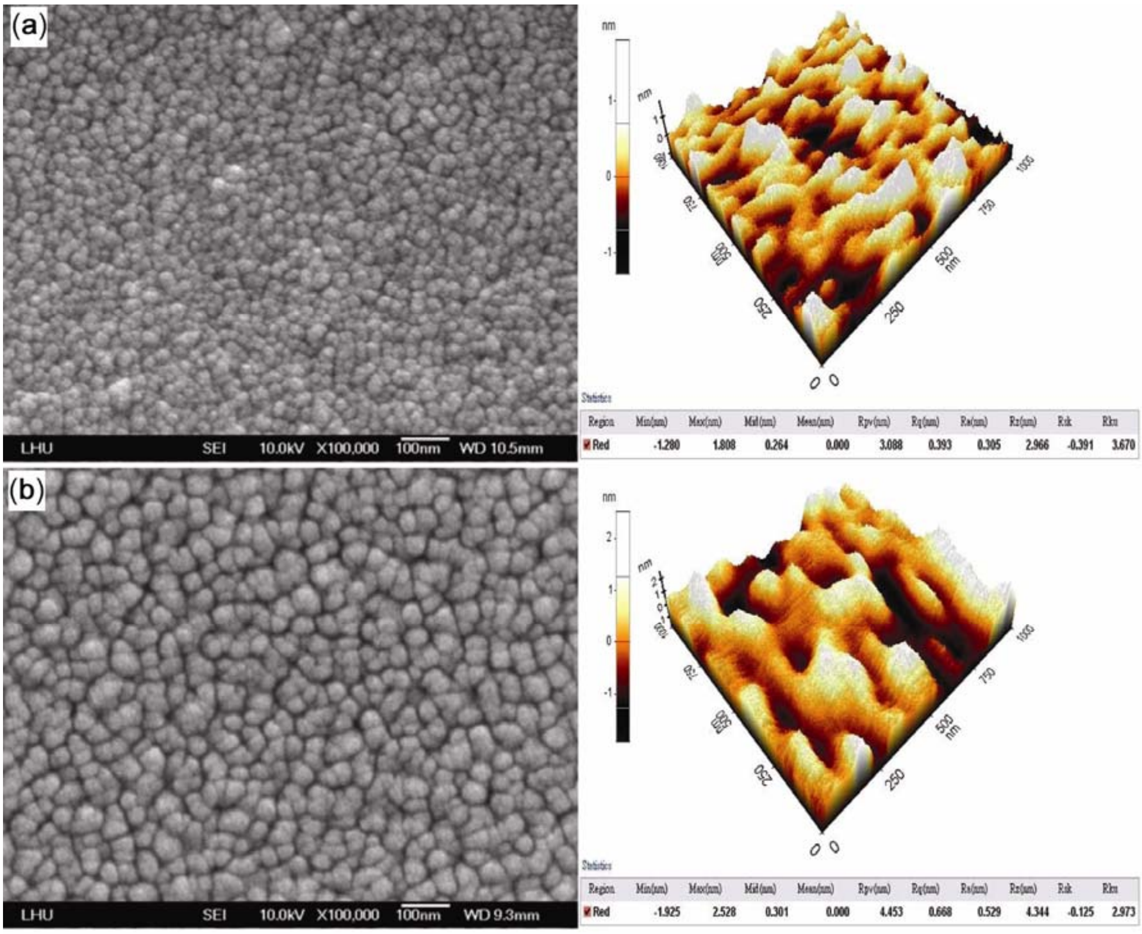

Figure 4. SEM (left) and AFM (right) images of the films corresponding to figure 2: (**a**) orthogonal array parameters (surface roughness of $R_a = 0{\cdot}305$ nm) and (**b**) grey theory prediction design ($R_a = 0{\cdot}529$ nm).

Table 6. Results of ANOVA for the grey relational grade in the AZO grown.

Factors	*S*/*N* ratio (dB) Level 1	Level 2	Level 3	Degree of freedom	Sum of square	Contribution Variance	(*P*%)
A	–3·003	–5·508	–6·905	2	23·45	11·73	66·35
B	–6·422	–3·889	–5·105	2	9·63	4·82	27·26
C	–5·279	–4·869	–5·267	2	0·33	0·17	0·96
D	–5·709	–5·130	–4·577	2	1·92	0·96	5·43
Total				8	35·33		100

2006). The surface roughness increases from $R_a = 0{\cdot}305$ to 0·529 nm, when grey theory prediction design is used.

4.2 *Effect of rf power and argon working pressure*

Table 6 shows the results of ANOVA for multiple performance characteristics of AZO grown. Using grey relational analysis, it can be seen that the rf power ($P = 66{\cdot}35\%$) strongly affects the multiple performance characteristics. In addition, working pressure also has some influence, with a contribution ratio of about 27·26%. When the working pressure (1 Pa), substrate temperature (90 °C) and deposition time (50 min) are constant, the rf power is varied between 30, 40, 50, 60 and 70 W, respectively (table 7). Figure 5(a) shows XRD patterns for AZO films grown on PET substrates as a function of rf power. All of the films display (0 0 2) peaks, which indicate that AZO films have a hexagonal ZnO wurtzite structure. An increase in rf power (from 30 to 70 W) produces a gradual decrease in FWHM of XRD for the AZO films. In figure 5(b), it is observed that using Taguchi experimental method the resistivity decreases when the rf power is

Table 7. Settings for rf power and working pressure.

Substrate	PET (T60, area 25 × 25 mm, thickness 1 mm)
Target	AZO ($ZnO : Al_2O_3$, 98 : 2 wt%, 99·995% pure)
Gas	Argon (99·995% purity)
Base pressure	$5{\cdot}3 \times 10^{-4}$ Pa
Substrate-to-target distance	90 mm
Substrate rotate speed	20 rpm
Substrate temperature	90 °C
Deposition time	50 min
Working pressure	1 Pa
rf power	30, 40, 50, 60, 70 W
rf power	50 W
Working pressure	0·9, 0·95, 1, 1·05, 1·1 Pa

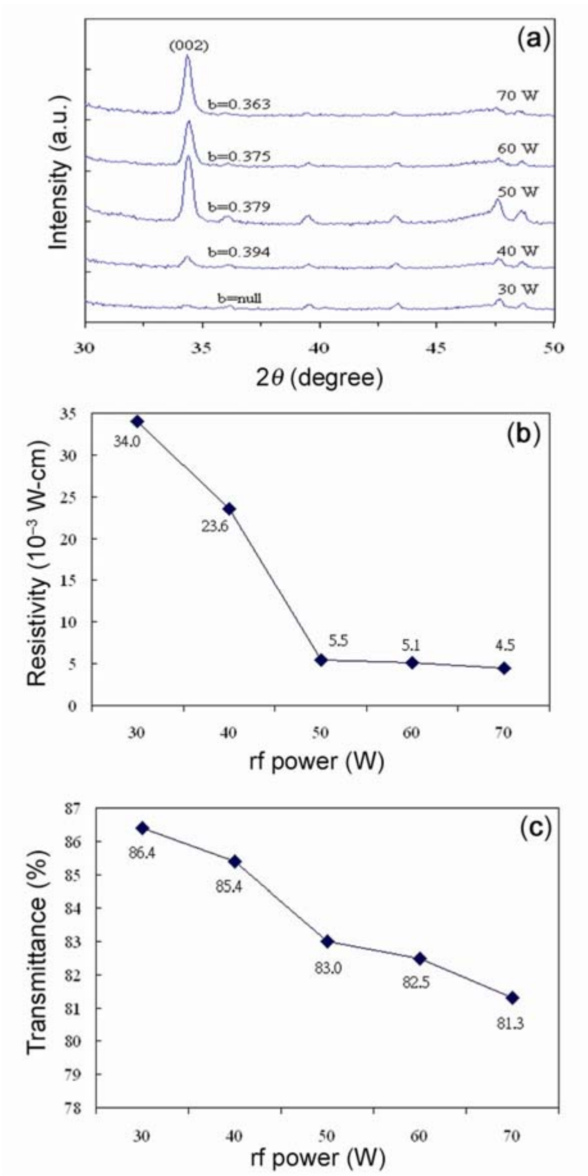

Figure 5. (**a**) X-ray curve, (**b**) electrical resistivity and (**c**) visible range transmittance, plotted as a function of rf power for AZO films grown on PET.

increased. The lowest resistivity of $4{\cdot}5 \times 10^{-3}$ Ω-cm is achieved at the highest rf power, 70 W. If the electron concentration is enhanced, the resulting resistivity is lower. The small amounts of Al_2O_3 doped into ZnO matrix to form AZO target provided excess electrons. The electrical nature of AZO films was affected by the extrinsic dopants (Chen and Duh 1991). This has been attributed to the changes in the stoichiometry and/or in the crystallinity of the films with the growth rate (Jeong and

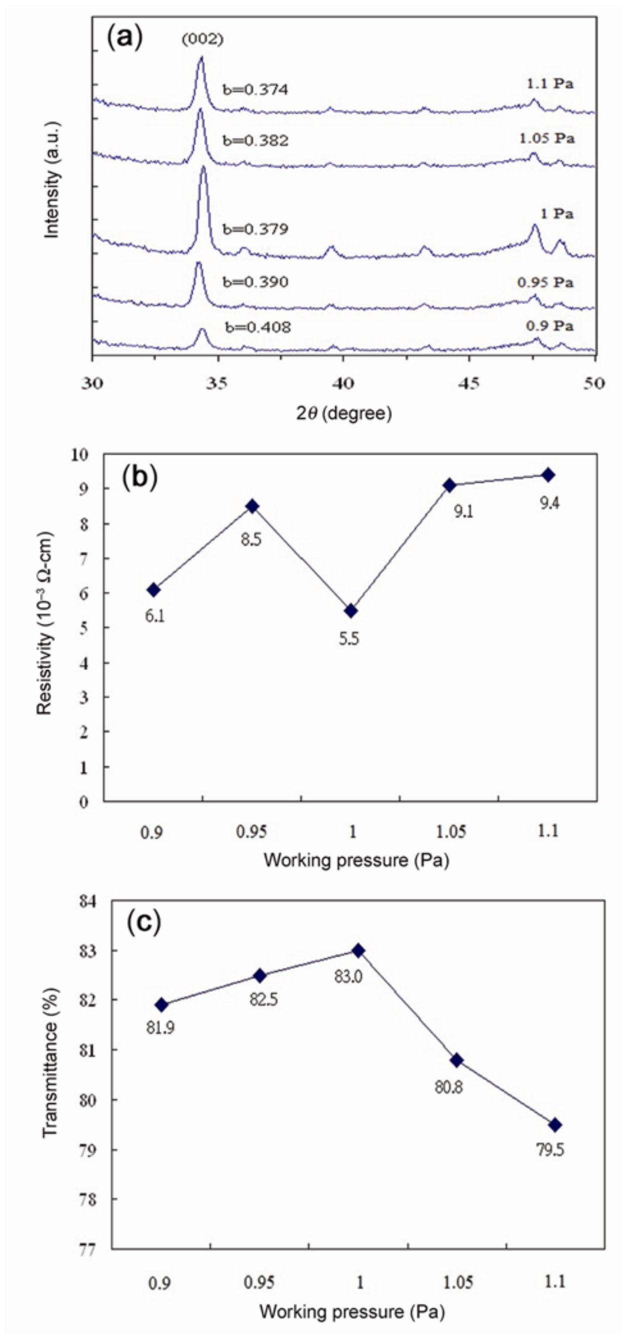

Figure 6. (**a**) X-ray curve, (**b**) electrical resistivity and (**c**) visible range transmittance, plotted as a function of working pressure, for AZO films grown on PET.

Boo 2004). However, the transmission spectrum for this sample is poor, showing an average transmission in the visible range of around 81·3% (figure 5c).

Figure 6(a) shows XRD patterns for the AZO films grown on PET substrates, as a function of working pressure. The (0 0 2) peak of X-ray curves is the highest at working pressure of 1 Pa. Using ANOVA analysis in table 3, rf power has the dominant effect on the deposition rate, with a contribution ratio of almost 95·29%, but the contribution ratio of working pressure is < 1·5%. This implied that the rate of deposition is the highest at working pressure of 1 Pa but the effect is not significant. The lowest resistivity and highest transmission are achieved at a working pressure of 1 Pa as well (figure 6(b) and (c)).

5. Conclusions

This study uses the Taguchi experimental design and grey relational analysis to clarify the influence of various process parameters on AZO/PET thin films using multiple performance characteristics. Experiments using an appropriate L_9 (3^4) orthogonal array and a Taguchi experimental design are conducted first. The experimental results are used to calculate the *S*/*N* ratio, the grades, in order to predict the optimal parameters using grey relational analysis. The electrical resistivity of the AZO/PET films is reduced from $2{\cdot}6 \times 10^{-2}$ to $5{\cdot}5 \times 10^{-3}$ Ω-cm and the visible range transmittance is > 83%, using the grey relational analysis. ANOVA for multiple performance characteristics shows that the rf power and working pressure have a dominant effect on AZO/PET electrical resistivity and visible transmittance, respectively. The results show that this method greatly simplifies the optimization of complicated multiple performance characteristics.

References

Agashe C, Kluth O, Hüpkes J, Zastrow U, Rech B and Wuttig M 2004 *J. Appl. Phys.* **95** 1911

Chen D Y and Hsu C Y 2008 *Superlattice Microst.* **44** 742

Chen Y I and Duh J G 1991 *Mater. Chem. Phys.* **27** 427

Chung Y M, Moon C S, Jung M J and Han J G 2005 *Surf. Coat. Technol.* **200** 936

Deng J L 1989 *J. Grey Syst.* **1** 1

Fernández S, Martínez-Steele A, Gandía J J and Naranjo F B 2009 *Thin Solid Films* **517** 3152

Fortunato E, Gonçalves A, Assunção V, Marques A, Águas H, Pereira L, Ferreira I and Martins R 2003 *Thin Solid Films* **442** 121

Hsu C Y and Tsang C H 2008 *Sol. Energ. Mater. Sol. Cells* **92** 530

Jeong S H and Boo J H 2004 *Thin Solid Films* **105** 447

Jin B J, Bae S H, Lee S Y and Im S 2000 *Mater. Sci. Eng.* **B71** 301

Kao J Y, Tsao C C, Wang S S and Hsu C Y 2010 *Int. J. Adv. Manuf. Technol.* **47** 395

Kassis A and Saad M 2003 *Sol. Energ. Mater. Sol. Cells* **80** 491

Kuo H H, Wu J H and Chin J 1998 *J. Grey Syst.* **1** 47

Lee J, Jung H, Lee J, Lim D, Yang K, Yi J and Song W C 2008 *Thin Solid Films* **516** 1634

Lin Y C, Chen M Z, Kuo C C and Yen W T 2009 *Colloids Surf. A: Physicochem. Eng. Aspects* **337** 52

Lv M, Xiu X, Pang Z, Dai Y and Han S 2006 *Appl. Surf. Sci.* **252** 5687

Miyazaki M, Sato K, Mitsui A and Nishimura H 1997 *J. Non-Cryst. Solids* **218** 323

Moon C S, Chung Y M, Jung W S and Han J G 2007 *Surf. Coat. Technol.* **210** 5035

Osama S M, Haitham R S and Hussam L A 2009 *Eng. Tech. J.* **27** 1143

Paraguay D F, Morales J, Estrada L W, Andrade E and Miki-Yoshida M 2000 *Thin Solid Films* **366** 16

Pei Z L, Zhang X B, Zhang G P, Gong J, Sun C, Huang R F and Wen L S 2006 *Thin Solid Films* **497** 20

Phillip J R 1989 *Taguchi techniques for quality engineering* (New York: McGraw-Hill)

Rim Y S, Kim S M, Choi H W, Park S J and Kim K H 2008 *Colloid. Surf.* **A313** 461

Szyszka B 1999 *Thin Solid Films* **351** 164

Tarng Y S, Juang S C and Chang C H 2002 *J. Mater. Process Technol.* **128** 1

Tseng C H, Huang C H, Chang H C, Chen D Y, Chou C P and Hsu C Y 2011 *Thin Solid Films* **519** 7959

Yu X, Ma J, Ji F, Wang Y, Zhang X, Cheng C and Ma H 2005a *Appl. Surf. Sci.* **239** 222

Yu X, Ma J, Ji F, Wang Y, Zhang X, Cheng C and Ma H 2005b *J. Cryst. Growth* **274** 474